Acta Technica *62* (2017), No. 6B, 849–860

A Practical Stability Control Method for Single-phase Inverter Circuit

Lin Jiang[1,2], Po Li[1,2*]

Abstract. This research puts forward a single-phase inverter circuit control method on the basis of the control of Lyapunov function for the purpose of practical stability guarantee to improve the application scope of the control method. Firstly, establish the precise digital model (small signal digital model) of single-phase inverter circuit under the circumstances of ignoring the unknown inputs and construct Lyapunov function based on passivity; secondly, taking inputting finite sets into account, deduce a method of determining the condition time based on Lyapunov function and theoretically guarantee the practical stability of deduction system in the time of the given sampling. Finally, conduct simulation and experimental verification for the feasibility of the proposed method.

Key words. Practical stability, Single-phase inverter circuit, Differential Lyapunov function, Stability control.

1. Introduction

With the rapid development of power electronics technology and the improvement of the performance requirements of electrical equipment in various industries, the application of inverter technology in many fields is becoming more and more extensive; consequently, the performance requirements of inverter power supply are getting higher and higher. Nowadays, lots of electrical equipment in many industries does not directly use the alternating current provided by the power grid as a power supply, but transforms the alternating current through various forms, so as to get all required electric energy forms. Some important power sectors and electricity equipment, especially the aerospace and ships have higher and higher requirements for power supply quality, which require accurate and good voltages, frequencies, waveforms, high dynamic performances, undisturbed power grids and clean or purified power supply conditions.

[1]School of Aerospace Engineering, Xiamen University, 361005
[2]Shenzhen Research Institute of Xiamen University,518000

Due to the fact that the power supply load increases but the capacity of a single power component is limited, it has been a trend of the current inverter power supply system design to parallel multiple inverter power supplies so as to increase system capacity and improve system reliability. It has a wide application prospect in the fields of aerospace, large computer power supply system, communication power supply system and bank power supply system, which have high requirements for the reliability of the power supply. The parallel operation of the inverter power supply mainly has three benefits as follows: firstly, when multiple power modules are connected in parallel, the average load power can be reduced, the load power can be borne averagely, which can reduce the current stress of main power devices in each module and is beneficial to the choice of power devices. Secondly, the reliability of operation can be improved by forming the parallel redundant system; when the power supply system consisting of inverter power supply modules is operated in redundant parallel mode, and any module in the system fails to work due to a fault, the remaining modules can continue to provide the load power, which greatly improves the reliability of the system. Thirdly, replacing serialization with modularization can form a variety of power levels of the power system flexibly and improve the standardization of the power module so as to shorten development and production cycle, reduce costs, and improve system maintainability and interchangeability. In addition, the development of distributed power supply system provides a broad application space for the inverter parallel technology. Compared with the centralized power supply, the distributed power supply system is arranged in the vicinity of the user in small size, decentralized manner, which can independently output electric energy, as a useful supplement to the large power grid. Especially when the large power grid is paralyzed, it will cause a huge loss of electricity, and power interruption will cause a series of chain reaction and bring significant losses to the national economy. However, the distributed power supply, because of its small size, even if it fails to supply power, will only cause a few direct and indirect losses. It has a bit influence factors of its safe operation and easy to control. What's more, the current wind energy, solar energy and other clean energy still do not have a larger scale, so that when the centralized power supply can not be realized, how to exert the advantages of power supply system to enhance the energy comprehensive utilization level is a subject that gains more and more attention. The inverter parallel control technology connecting the distributed inverter organically and forming a network power supply system model has the engineering application value; thereby, the parallel control technology of single-phase inverter system will be studied deeply in this paper.

2. Mathematical model construction of single - phase inverter circuit by inputting finite sets

Figure 1 shows a typical single - phase inverter circuit model in the form of resistance-inductance load, where i_L represents the current flowing through the inductor, taking the direction of the arrow as the positive direction; R represents the load resistance of the system circuit; U represents direct current input power supply.

Such a single-phase inverter circuit system model can be expressed as follows:

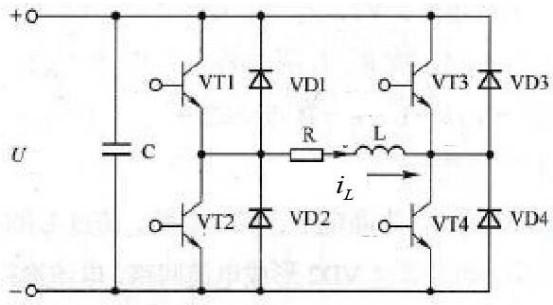

Fig. 1. A typical single - phase inverter circuit model in the form of resistance-inductance load

$$\frac{di_L}{dt} = \frac{1}{L}(U - i_L R) \text{ (switch } VT_1VT_4 \text{ is open, } VT_2VT_3 \text{ is closed)}. \tag{1}$$

$$\frac{di_L}{dt} = \frac{1}{L}(-U - i_L R) \text{ (switch } VT_2VT_3 \text{ is open, } VT_1VT_4 \text{ is closed)}. \tag{2}$$

Introduce the input parameter S to represent the opening and closing condition of the switch $VT_1VT_2VT_3VT_4$(where $S = 1$ represents that the switch VT_1VT_4 is open and VT_2VT_3 is closed, $S = -1$ represents that the switch VT_2VT_3 is open and VT_1VT_4 is closed), therefore, combine the formula (1)with (2) to form the mathematical model of single - phase inverter with switching states, which can be expressed as follows:

$$\frac{di_L}{dt} = \frac{1}{L}(US - i_L R). \tag{3}$$

In the formula (3), the parameter S can only be -1 or 1, namely, the characteristic of the inverter circuit itself determines that it is a limited input system with two input states. Copy the formula (3) and make it as the target observer model. Meanwhile, introduce the symbol * to represent the target parameters of tracking during the working process of DC-AC single-phase full-bridge inverter circuit. Make $i_L^* = A\sin(\omega t + \phi)$ be available for the reference value equation of the parameter and be available for the tracking of the parameter i_L in the following deduction. Equation (4) lists the target reference value model.

$$A\omega\cos(\omega t + \phi) = \frac{di_L^*}{dt} = \frac{1}{L}(US^* - i_L^* R). \tag{4}$$

Subtract the formula (4) from the formula (3) to obtain the error value model based on the input state, at the same time, we replace x_1 with i_L for the convenience of expression and obtain the formula (5) as follows:

$$\frac{d\widetilde{x_1}}{dt} = \frac{1}{L}[U(S - S^*) - \widetilde{x_1}R]. \tag{5}$$

Where $\widetilde{x_1} = x_1 - x_1^*$, $S - S^* \in \{-1 - S^*, 1 - S^*\}$ in the formula (5) and$S^* \in [-1, 1]$, which has been mentioned above (only take the two ends of the interval at the position of several discrete points) are in a finite input state set.

Constructing Lyapunov function $V = \frac{1}{2}L\widetilde{x_1}^2$ in continuous model by selecting the form of similar energy function, the derivative of the Lyapunov function is expressed as follows:

$$\dot{V} = [U(S - S^*) - \widetilde{x_1}R]\widetilde{x_1} = U(S - S^*)\widetilde{x_1} - \widetilde{x_1}^2 R\,. \tag{6}$$

$S^* = \frac{A\sin(\omega t+\phi)R + A\omega L\cos(\omega t+\phi)}{U} = \frac{A\sqrt{R^2+(\omega L)^2}\sin(\omega t+\phi')}{U} \in [-1, 1]$ is a triangular form, but the values of $S - S^*$ are still a non-positive and a non-negative value at any time, it can be seen that if we choose $S - S^*$ at every moment and make $S - S^*$ and $\widetilde{x_1}$ have the opposite sign or be 0 (a point equal to 0 is discontinuous, which will not affect its progressive stability), what's more, the second item itself is non-positive, then $\dot{V} \leq 0$ will be guaranteed at any time, the continuous model of this system is stable according to the Second Theorem of Lyapunov Stabilization.

3. Practical stability analysis of single - phase inverter circuit

In order to facilitate the expression of subsequent equations, introduce the parameter $\widetilde{S}$ to replace $S - S^*$. Before examining the stability of the system, we need to discretize the state space model of the system. We use the postfix notation of $(k+1)$ and (k) to represent the parameter state of single-phase inverter circuit of the moment of $(k+1)\,T_s$ and kT_s respectively and use T_s to represent the sampling time of the system. Then the discretization equation of equation (5) is obtained and expressed as follows:

$$\widetilde{x_1}\,(k+1) = \frac{T_s}{L}U\widetilde{S}\,(k) - \frac{T_s}{L}\widetilde{x_1}\,(k)\,R + \widetilde{x_1}\,(k)\ . \tag{7}$$

Use Lyapunov Function in analogical continuity model to construct Lyapunov Function $V\,(k) = \frac{1}{2}L\widetilde{x_1}\,(k)^2$ in discrete system so as to describe the entire steady state. Lyapunov function differential function after discretization can be expressed as:

$$\begin{aligned}\Delta V &= V\,(k+1) - V\,(k) = \frac{1}{2}L\widetilde{x_1}\,(k+1)^2 - \frac{1}{2}L\widetilde{x_1}\,(k)^2 \\ &= \frac{1}{2}L\left[\frac{T_s}{L}U\widetilde{S}\,(k) - \frac{T_s}{L}\widetilde{x_1}\,(k)\,R + \widetilde{x_1}\,(k)\right]^2 - \frac{1}{2}L\widetilde{x_1}\,(k)^2 \\ &= \frac{T_s^2}{2L}\left[U\widetilde{S}\,(k) - \widetilde{x_1}\,(k)\,R\right]^2 + T_sU\widetilde{S}\,(k)\,\widetilde{x_1}\,(k) - T_s\widetilde{x_1}\,(k)^2\ .\end{aligned} \tag{8}$$

The formula (8) is very complicated, but we can get some useful conclusions by carefully analyzing its expressions: first of all, the latter two expressions of equation (8) are similar to the derivative form of the Lyapunov function in continuity system model, the polynomial $T_sU\widetilde{S}\,(k)\,\widetilde{x_1}\,(k)$ can similarly control and guarantee that $S -$

S^* and $\widetilde{x_1}$ have the opposite sign and is non-positive definite at any time and the third polynomial is non-positive definite. In addition we can find that if we choose enough small T_s, that is the sampling time is short enough, the first two nonnegative definite items will not produce too large influence on the whole system when the system is not close to the equilibrium position. So if we choose a relatively small sampling frequency, the system will control the non-positive of Li Yapunov function in a wide range to form a situation of converging to a stable point. But we find that there is a certain stability problem in the vicinity of the stability point, because in a small range interval around a stable point, no matter how the switch input situation is chosen, the difference function of the Lyapunov function of the system function can not be guaranteed as the non-positive definite. Then we need to examine the specific circumstance of the differential function and describe the "dead region" of the difference function (namely, the function can not guarantee the non-positive definite region). In order to analyze this differential function in detail, we define that when $S = -1$, $\Delta V = f_1$ and when $S = 1$, $\Delta V = f_2$ to facilitate the subsequent expression. Considering that the form of function (8) is complex, we examine the critical situation $\Delta V = 0$ of $S = -1$ and $S = 1$ respectively and take the curve $\Delta V = 0$ as a boundary to divide the plane $\widetilde{x_1}t$ into multiple regions to discuss. If figure 2 is under the curvef_1, $f_1 > 0$; otherwise, $f_1 < 0$. Similarly, if figure 2 is under the curve f_2, $f_2 > 0$; otherwise, $f_2 < 0$. Provided that the maximum value of V is E_Ω when using $\Delta V = 0$ to surround Ω region and the maximum ΔV of a sampling period starting from Ω region is ΔE_T; all alternative inputs of the control rate make $\Delta V \geq 0$ so that to keep the input guarantee of the last sampling cycle invariable when inputting $\widetilde{S}$ in Ω region guarantees that ΔV is the continuous function relevant to $\widetilde{x_1}$ and there is maximum value $\Delta V_{\max}$ in bounded closed region Ω. The maximum value of V leaving Ω region is $E_\Omega + \Delta E_T < E_\Omega + \Delta V_{\max} T_s$. Provided that Θ is the oval region surrounded by $V = E_\Omega + \Delta V_{\max} T_s$, model consistence practice of the single-phase inverter circuit lies in Θ region steadily according to the practical stability definition.

The switch state can not be changed within a sampling period, so function control requires switching and the control can not be adjusted real-time and the state $\Delta V > 0$ appears, which a common phenomenon in universal control method. But we can find that it can be corrected in time when being unable to pass the next round within Ω region. So, we can not keep the control of the system function near the ideal origin within Ω region (full real-time tracking). On the other hand, there may be the circumstance that when a certain switch state just enters Ω region but does not pass through the region and ends the control cycle in the middle of the region, we need to keep the control rate to the next cycle until it leaves the region completely and leaving is bound to be guaranteed. Because two switch states within Ω region make $\Delta V > 0$, no matter which state we choose, the system will make the parallel line formed by the selected function $V(k) = \frac{1}{2} L\widetilde{x_1}(k)^2$ move forward to the parallel line with larger and larger area until leaving Ω region(where the critical state is the intersection of oval of $V(k) = \frac{1}{2} L\widetilde{x_1}(k)^2$ and Ω region, and if $V(k) = \frac{1}{2} L\widetilde{x_1}(k)^2$ increases a small amount, the intersection will not exist.)

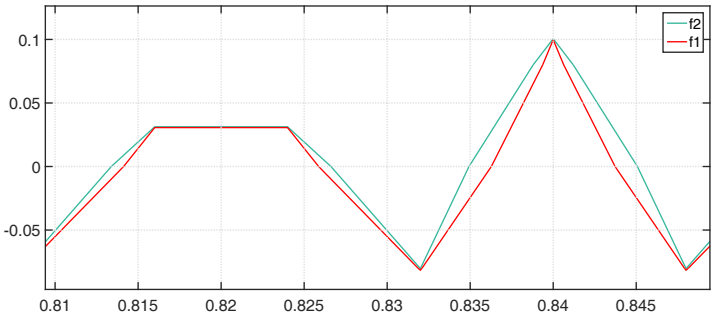

Fig. 2. Current bias near target origin of single-phase inverter circuit changing with time when $\Delta V = 0$

4. Simulation and experimental results of single - phase inverter circuit

The relevant parameters of the single-phase inverter circuit simulation are listed in table 1, and the Simulink simulation block diagram of the single-phase inverter circuit is shown in Fig. 3.

Table 1. Simulation test parameters of single- phase full bridge inverter circuit

Load Resistance R(Ω)	10
Load inductance L(H)	0.01
Input voltage U(V)	5
Control frequency(kHz)	40

(1) Practical stability simulation

We set the tracking target as $0.1 * \cos(100\pi t)A$, the tracking effect is shown as figure 3 and figure 4. Based on the simulation results of a large number of different parameters, we find that changing the inductance parameter and the control frequency will make an effect on the simulation result. It is also worth mentioning that the practical stability can also be achieved be a large number of simulation tests to track relatively small current in the group of simulation parameters.

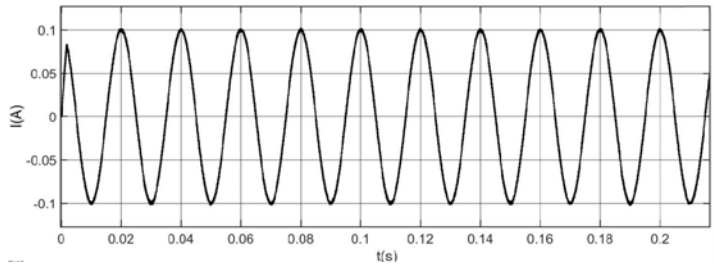

Fig. 3. Current tracking result of system tracking voltage $0.1 * \cos(100\pi t)A$

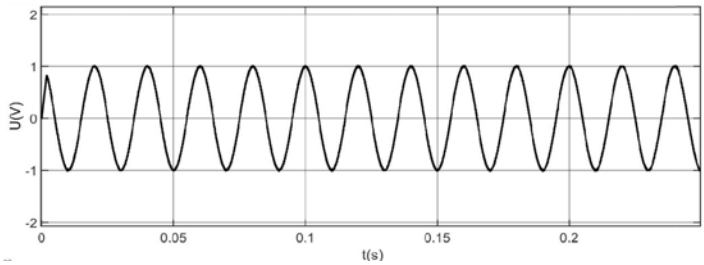

Fig. 4. Current tracking result of system tracking voltage $0.1 * \cos(100\pi t)A$

(2) Dynamic performance simulation

Figure 3.18 and figure 3.19 show the dynamic characteristics of the control rate under the single-phase inverter circuit. In the process of Simulink simulation, applying a current disturbance additionally when the simulation time is 1s and lowering the tracking current from $0.1 * \cos(100\pi t)A$ to $0.05 * \cos(100\pi t)A$, we find that the dynamic characteristics of the control rate under the single-phase inverter circuit is satisfactory basically. A large number of tests show that if the actual inductance is small, the dynamic characteristics will be significantly improved.

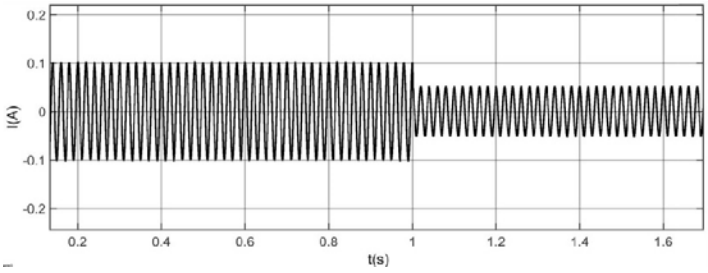

Fig. 5. Current tracking result of system tracking voltage $0.05 * \cos(100\pi t)A$ when changing from $0.1 * \cos(100\pi t)A$ at 1s

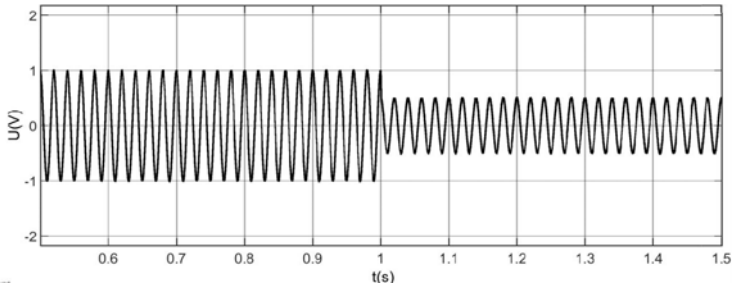

Fig. 6. Current tracking result of system tracking voltage $0.05 * \cos(100\pi t)A$ when changing from $0.1 * \cos(100\pi t)A$ at 1s

(3) Relationship between control frequency and control error

According to the previous study, the switch status can not be adjusted immediately, therefore a situation where $\Delta V > 0$ within a control period forms. In the

"dead region" of system control, maybe there is $\Delta V > 0$ in a variety of options. According to equation (8) we can deduce that when $\Delta V = 0$, the control frequency meets $T_s{=}2L\frac{U\widetilde{S}(k)\widetilde{x_1}(k)-\widetilde{x_1}(k)^2}{\left[U\widetilde{S}(k)-\widetilde{x_1}(k)R\right]^2}$ (the value of $\widetilde{S}$ ensures that the first item of the denominator can not be 0, it can do division when denominator is not 0), from which we can see that the control frequency affects the size of Ω region that is affecting the size of E_Ω. The changeable ΔE_T of each control cycle is directly affected by the control frequency and makes a great effect on the size of Θ region, so it can be concluded that the control frequency has a large influence on the control error. In order to study the correlation between its effects, this text uses statistical methods; under the circumstances that the duration from system start-up to that the system enters required practical stability state can not be judged, the text chooses to extend the simulation time to be long enough (8000 control cycles) and take 20% of the time data as samples to analyze after determining the simulation time. Select class energy function J to evaluate the control error and examine the deviation of practical stability, get the maximum value under the control error indicator of the sampling datum under different sampling frequencies and judge whether the control frequency can be accepted.

$$J = \frac{1}{2}L\widetilde{x_1}^2. \tag{9}$$

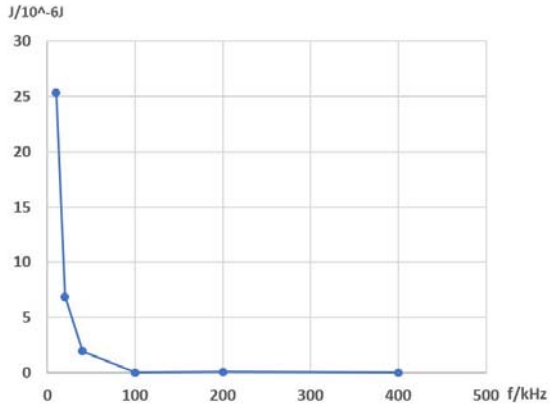

Fig. 7. Corresponding errors of different control frequencies under simulation test

Table 2. Corresponding control errors of different control frequencies under simulation test

Control frequency /kHz	Control error /10^-6J
400	0.020400
200	0.080912
100	0. 31963
40	1.9486
20	6.8880
10	25.331

Table 3.2 and table 3.10 show the relationship between control errors and control frequencies. It can be found that they have a negative correlation. A large number of simulation tests can prove that if the frequency is lower than the simulation parameters listed in table 3.1, the uncontrolled state will appear and the control deviation of 10kHz and 20kHz will become relatively large. Under the existing experimental conditions, it is relatively reasonable and effective to set the simulation as 40kHz.

(4) Experimental results

Based on the platform of CompactRIO 9073-FPGA, using LabVIEW 2012 to conduct up and down programming, the experimental parameters are listed in table 3.

Table 3. Experimental test parameters of single-phase full bridge inverter circuit

Load Resistance R(Ω)	4
Load inductance L(H)	0.01
Input voltage U(V)	12
Control frequency(kHz)	40

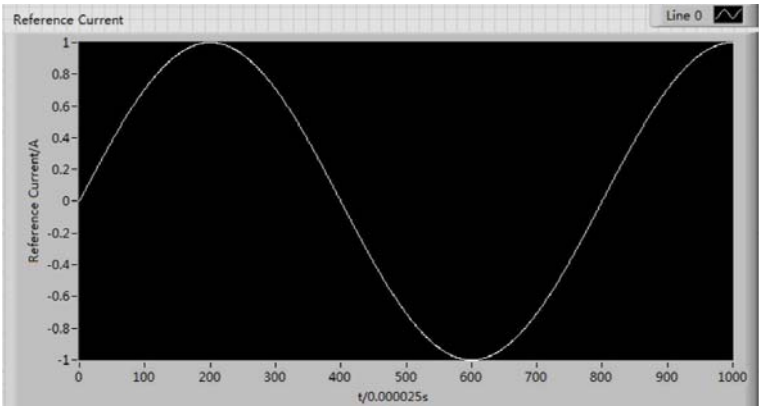

Fig. 8. Experiment current waveforms to be tracked $1 * \cos(100\pi t)A$

The experimental results are shown in figure 8, figure 9 and figure 10. Under the circumstances of tracking $1 * \cos(100\pi t)A$, the system presents a very good practical stability effect, and has tracked the current waveforms well, which is similar with simulation results.

5. Conclusion

In this part of the study, we examine the single-phase inverter circuit system practical stability control method. We design the control rate based on making the discretization energy function as the control Lyapunov function, and finally obtain

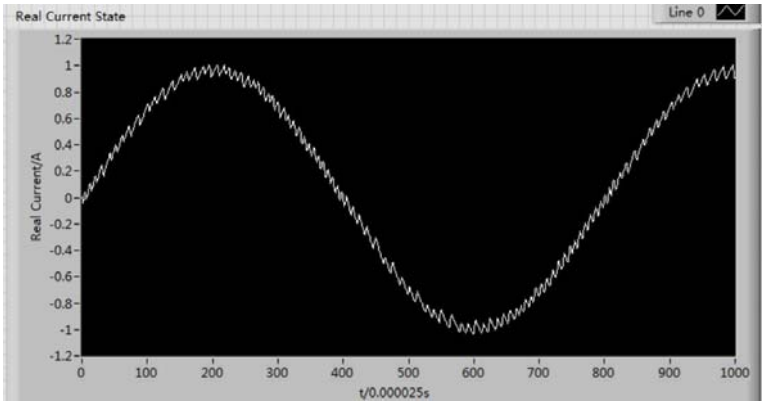

Fig. 9. Experiment actual tracking current waveforms $1 * \cos(100\pi t) A$ effect

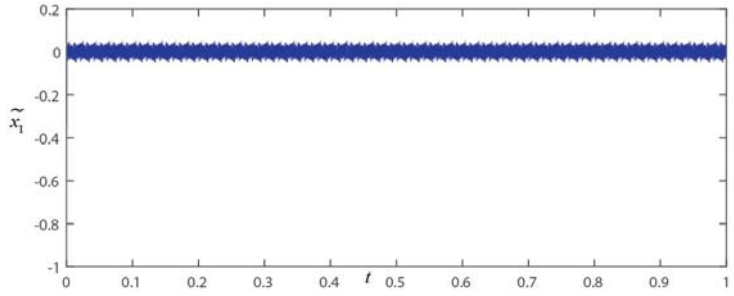

Fig. 10. Current tracking difference situation showing a practical stability

the corresponding conclusion under the simulation test.

In order to study this complex state process, we draw cross-section lines with Matlab to analyze the specific situation of ΔV and obtain the class energy distribution. We get the following conclusions according to the simulation:

(1) Based on the fact that the input is a finite set and the input state model construction shall b considered, we select the appropriate sampling frequency and switch state to control the single-phase inverter circuit to achieve its practical stability, and the control strategy sources from discretization construction class energy function of Lyapunov function.

(2) In order to carry out the simulation in the single-phase inverter circuit, we need to select the reference amount. Whenever a current reference is selected, the corresponding switch reference status is obtained. The actual simulation results show that the practical stability can meet certain needs under certain operating conditions, which does not need strict and progressive stability guarantee. Nonetheless, the parameters of the system itself have other effects on the performance of the control strategy under the single-phase inverter circuit.

(3) The control frequency will make a great impact on the control error, showing a negative correlation. Therefore, if we increase the control frequency as much as possible, the system control error will be improved well.

Acknowledgements

This work was supported by Nature Science Foundation of Shenzhen City, China (JCYJ20160530173515852)

References

[1] Abdel-Rahim N, Quaicoe J E: (1994) *Multiple feedback loop control strategy for single-phase voltage-source UPS inverter*[C]// Power Electronics Specialists Conference, Pesc '94 Record. IEEE. IEEE, 1994:958-964 vol.2.

[2] Hoang K D, Zhu Z Q, Foster M: (2013) *Direct torque control of permanent magnet brushless AC drive with single-phase open-circuit fault accounting for influence of inverter voltage drop*[J]. Iet Electric Power Applications, 7(5):369-380.

[3] Dahono P A, Ismutadi P, Sato Y, et al.: (2001) *A control method for single-phase PWM inverters*[C]// IEEE International Conference on Power Electronics and Drive Systems, 2001. Proceedings. IEEE, 2001:282-285 vol.1.

[4] Abdel-Rahim N, Quaicoe J E: (1993) *Indirect current control scheme for a single-phase voltage-source utility interface inverter*[C]// Electrical and Computer Engineering, 1993. Canadian Conference on. IEEE, 1993:305-308 vol.1.

[5] Takamatsu S, Shimada E, Yokoyama T: (2009) *Digital Control Method for Single Phase Utility Interactive Inverter Using Deadbeat Control with FPGA Based Hardware Controller*[C]// Power Electronics and Motion Control Conference, 2006. Epe-Pemc 2006. International. IEEE, 2009:1436-1441.

[6] Sahu P K, Maity S, Mahakhuda R K, et al.: (2015) *A fixed switching frequency sliding mode control for single-phase voltage source inverter*[C]// International Conference on Circuit, Power and Computing Technologies. IEEE, 2015:1006-1010.

[7] Ufnalski B, Grzesiak L M: (2014) *A plug-in direct particle swarm repetitive controller for a single-phase inverter*[J]. Przeglad Elektrotechniczny, 90(6):6-11.

[8] Yu J, Cao Y, Min H, et al.: (2013) *Maximum power point tracking method for single-phase single-stage photovoltaic inverter*[J]. Chinese Journal of Scientific Instrument, 34(1):18-25.

[9] Wang W, Yan L, Zeng X, et al.: (2017) *Principle and Design of a Single-Phase Inverter-Based Grounding System for Neutral-to-Ground Voltage Compensation in Distribution Networks*[J]. IEEE Transactions on Industrial Electronics, 64(2):1204-1213.

[10] Noge Y, Itoh J I: (2012) *Multi-level inverter with H-bridge clamp circuit for single-phase three-wire grid connection suitable for Super-junction/SiC MOSFET*[C]// Power Electronics and Motion Control Conference. IEEE, 2012:88-93.

[11] Liang B, Wen-Long Q U: (2006) *A new control method for parallel single-phase DC/AC inverter*[J]. Advanced Technology of Electrical Engineering & Energy, 25(4):58-62.

[12] Yue Z, Tan J F: (2010) N*ew method for constant-frequency hysteresis current control of single phase grid-connected inverter*[J]. Chinese Journal of Power Sources, 34(1):66-69.

[13] Takeuchi S, Wada K: (2016) *Current Control of a Single-Phase Inverter by Applying a Multisampling Method*[J]. Electronics & Communications in Japan, 99(12):44-53.

[14] Hayashi K, Takamatsu S, Yokoyama T: (2007) *Precise digital control method with sinusoid based model for single phase utility interactive inverter with FPGA based hardware controller*[C]// European Conference on Power Electronics and Applications. IEEE Xplore, 2007:1-8.

Received May 7, 2017